

Supporting information for:

Green fluorescent genetically encoded calcium indicator based on calmodulin/M13-peptide from fungi

Natalia V. Barykina^{1,2}, Oksana M. Subach^{1,3}, Kiryl D. Piatkevich⁴, Erica E. Jung⁴, Aleksey Y. Malyshev⁵, Ivan V. Smirnov^{5,6}, Andrey O. Bogorodskiy¹, Valentin I. Borshchevskiy¹, Anna M. Varizhuk^{7,8}, Galina E. Pozmogova⁷, Edward S. Boyden^{4,9}, Konstantin V. Anokhin^{2,3,10}, Grigori N. Enikolopov^{1,11,12*}, & Fedor V. Subach^{1*}

¹Moscow Institute of Physics and Technology, Dolgoprudny, Moscow Region, Russia

²P.K. Anokhin Institute of Normal Physiology of RAMS, Moscow, Russia

³National Research Center "Kurchatov Institute", Moscow, Russia

⁴MIT Media Lab, Massachusetts Institute of Technology, Cambridge, MA, USA

⁵Institute of Higher Nervous Activity and Neurophysiology of RAS, Moscow, Russia

⁶Medico-Biological Faculty, N.I. Pirogov Russian National Research Medical University, Moscow, Russia

⁷Federal Research and Clinical Center of Physical-Chemical Medicine of Federal Medical Biological Agency, Moscow, Russia

⁸Engelhardt Institute of Molecular Biology RAS, Moscow, Russia

⁹MIT McGovern Institute for Brain Research, MIT, Cambridge, MA, USA

¹⁰Lomonosov Moscow State University, Moscow, Russia

¹¹Department of Anesthesiology, Stony Brook University Medical Center, NY, USA

¹²Center for Developmental Genetics, Stony Brook University, NY, USA

*Correspondence and requests for materials should be addressed to F.V.S. (email: subach.fv@mipt.ru) or G.N.E. (email: Grigori.Enikolopov@stonybrookmedicine.edu)

S1 Supporting information

Figure A. Alignment of the amino acid sequences for CaMs and peptides from CaM-dependent kinases and calcineurins found in different species.

Figure B. Alignment of the amino acid sequences for original library and FGCaMP calcium indicator.

Figure C. pH dependence of absorbance for the purified FGCaMP indicator.

Figure D. Size-exclusion chromatography for FGCaMP protein.

Figure E. Ca^{2+} titration curves for FGCaMP and GCaMP6s in the absence or presence of 1 mM MgCl_2 .

Figure F. Kinetic curves obtained from Ca^{2+} -association experiments.

Figure G. Detailed analysis of the onset kinetics for Ca^{2+} -binding.

Figure H. Alignment of the amino acid sequences of M13-like peptides and CaMs from FGCaMP and the other calcium indicators.

Figure I. Ca^{2+} titration curves for FGCaMP mutants.

Figure J. Ca^{2+} titration curves for FGCaMP2 mutants with mutations in CaM part.

Figure K. Ca^{2+} titration curves for FGCaMP3 variants with mutations in the M13-like peptide.

Figure L. Reversible changes in the mobile fraction of the FGCaMP indicator at the transition from high to low Ca^{2+} concentrations in HeLa Kyoto cells studied by FRAP experiments.

Figure M. Fluorescence changes in response to the external electric field in cultured neurons expressing FGCaMP indicator.

Figure N. confocal ratiometric calcium imaging with FGCaMP during 4-AP induced neuronal activity in paralyzed larvae embedded in ultra-low-melting agarose gel.

Figure O. Lightsheet ratiometric calcium imaging with FGCaMP during 4-AP induced neuronal activity in paralyzed larvae embedded in ultra-low-melting agarose gel.

Table A. Brightness and contrasts for FGCaMP and other ratiometric green and yellow GECIs.

Table B. K_d values and fluorescence contrasts for 402- and 493-forms of FGCaMP and its mutants.

Table C. List of primers.

A

```
A.niger      1: MADS L TEE Q VSEY KEAFSLFDK DGDG Q I T T K E L G T V M R S L G Q N P S E S E L Q D M I N E V L A D N 60
K.pastoris  1: M S D K L S F A Q I S E F K E A F S L F D Q D D G K I T S K E L G I V M R S L G Q T P T E S E L N D L I R E I D S N T 60
Mus.musculus 1: M A D Q L T E E Q I A E F K E A F S L F D K D G D G T I T T K E L G T V M R S L G Q N P T E A E L Q D M I N E V L A D G 60

A.niger      61: N G T I D F P E F L T M M A R K M K D T D S E E I R E A F K V F D R N N G F I S A A E L R H V M T S I G E K L T D D 120
K.pastoris   61: D G S I D F P E F L T M M A R K M R D S D S Q A E I F E A F R V F D K D G D G K I D K G E L K H V L T S I G E K L T E E 120
Mus.musculus 61: N G T I D F P E F L T M M A R K M K D T D S E E I R E A F R V F D K D G N G Y I S A A E L R H V M T N I G E K L T D E 120

A.niger      121: E V D E M I R E A D Q D G D G R I D Y N E F V Q I M M Q R 149
K.pastoris   121: E V D E M L R E A D T N N D G V I D I K E F S N L L V M K 149
Mus.musculus 121: E V D E M I R E A D I D G D G V N Y E E F V Q M M T A K 149
```

B

```
A. fumigatus 1: R R T L H K A I - D T V F A I N K L R E G 20
Chicken      1: R R K W Q K T G - H A V F A I G R L S S M 20
K. pastoris  1: - R S K F K Q V I E I V K M Q N R L K N L 20
Mus. musculus 1: R R K W Q K T G - N A V F A I G R L S S M 20
```

C

```
A. fumigatus 1: - K R R A - I K N K I L A I G F L S R V F Q V L R 23
K. pastoris  1: - K - K V V L R N K I L A I G F V S R M Y Q V L R 23
Mus. musculus 1: R K E V I R N - - K I R A I G F M A R V F S V L R 23
```

Figure A. Alignment of the amino acid sequences for CaMs and peptides from CaM-dependent kinases and calcineurins found in different species. (A) Alignment of the amino acid sequences for CaMs from *A. niger*, *K. pastoris*, and *M. musculus*. (B) Alignment of the amino acid sequences for M13-like peptides from CaM-dependent kinases from *A. fumigatus*, chicken, *K. pastoris*, and *M. musculus*. (C) Alignment of the amino acid sequences for calcineurins from *A. fumigatus*, *K. pastoris*, and *M. musculus*. Identical residues are selected with red boxes.

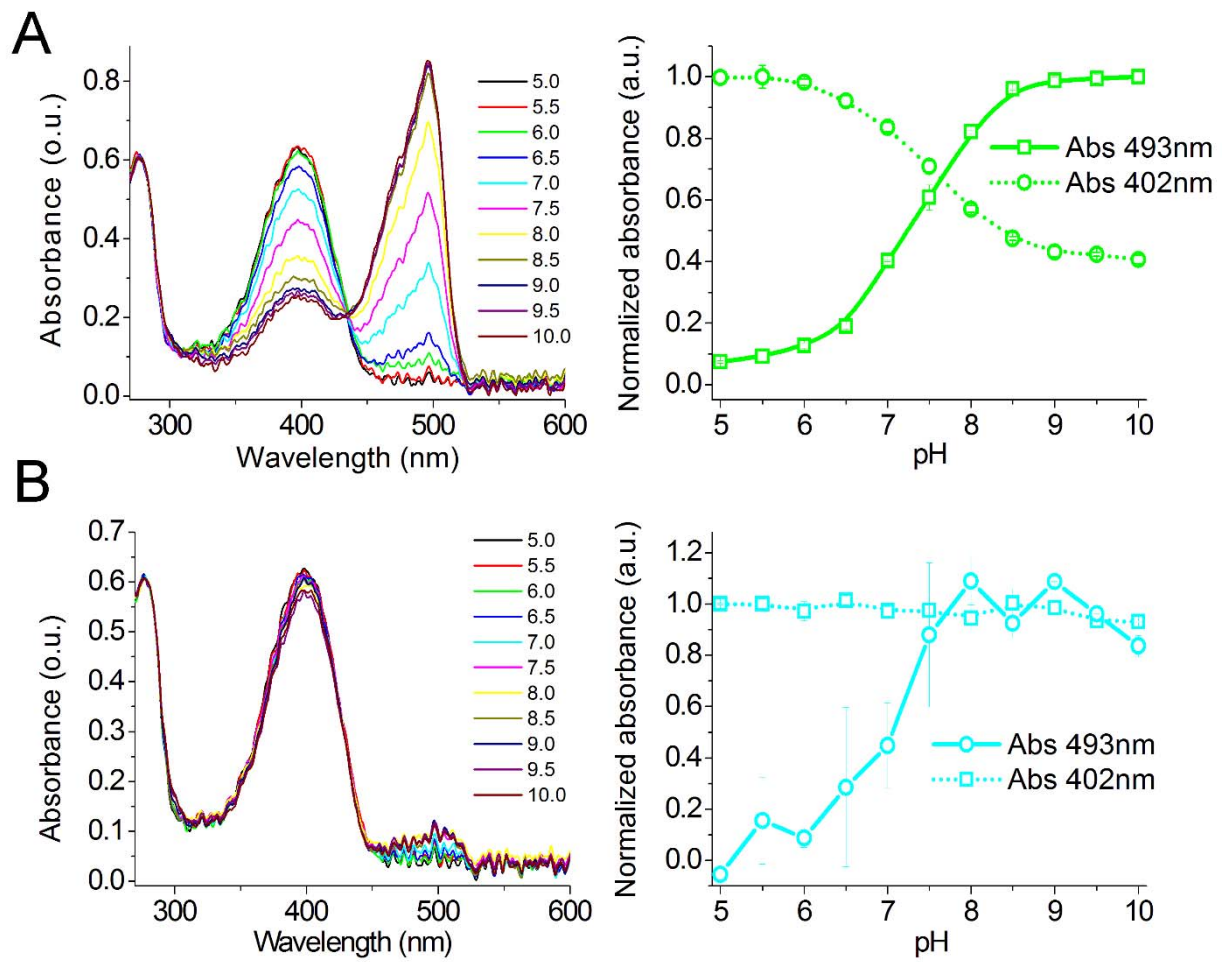


Figure C. pH dependence of absorbance for the purified FGCaMP indicator. (A, B) Absorbance spectra (left) and the normalized absorbance at 402 and 493nm (right) for FGCaMP in Ca²⁺-bound (A) and Ca²⁺-free (B) states in the range of pH values of 5-10. Error bars represent the standard deviation.

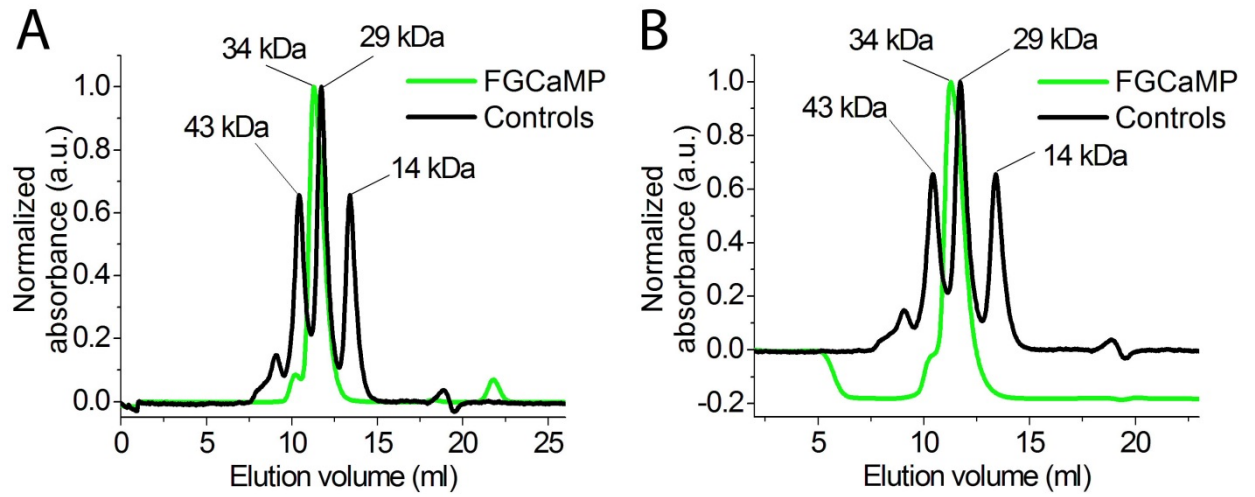


Figure D. Size-exclusion chromatography for FGCaMP protein. Fast protein liquid chromatography of FGCaMP in 20 mM Tris-HCl (pH 7.5), 200 mM NaCl buffer supplemented with 2 mM EDTA (A) or in 20 mM Tris-HCl (pH 7.5), 100 mM NaCl buffer supplemented with 1 mM CaCl_2 (B).

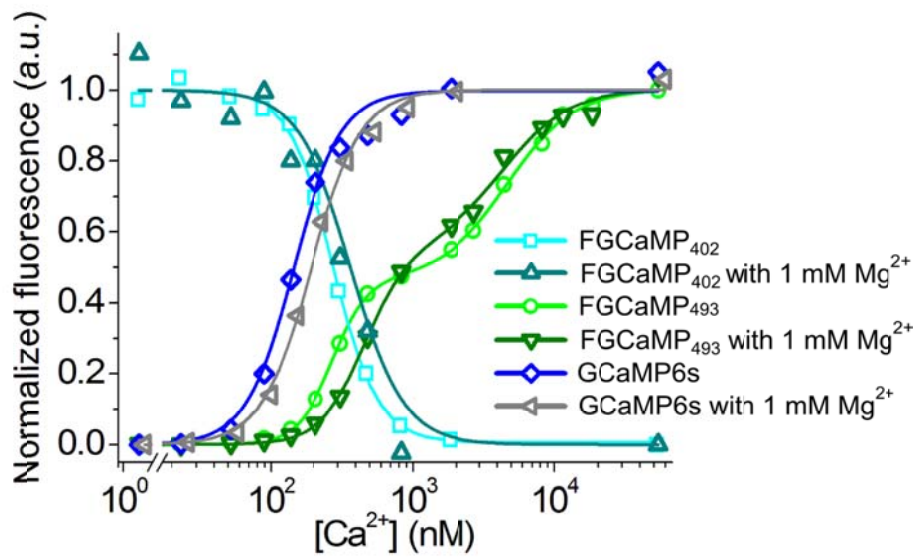


Figure E. Ca^{2+} titration curves for FGCaMP and GCaMP6s in the absence or presence of 1 mM MgCl_2 . Ca^{2+} titration curves for 402- and 493-forms of FGCaMP were acquired using 402 and 490 nm excitation light, respectively. Fluorescence changes were normalized to maximal and minimal values. Experimental data were fitted to Hill equation or double Hill equation $y = V_1 \cdot x^{n_1} / (K_{d1}^{n_1} + x^{n_1}) + V_2 \cdot x^{n_2} / (K_{d2}^{n_2} + x^{n_2})$, respectively.

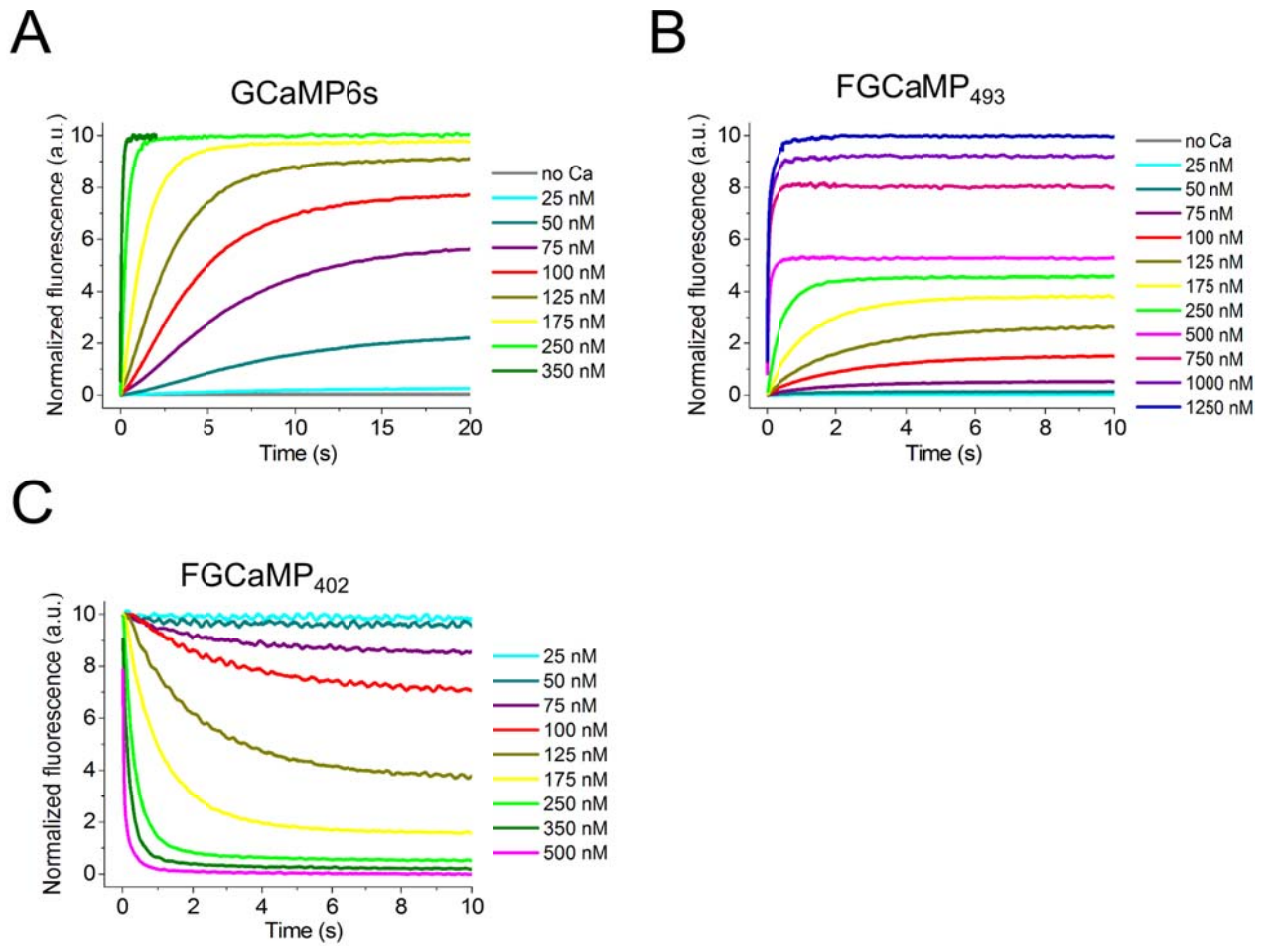


Figure F. Kinetic curves obtained from Ca^{2+} -association experiments. Fluorescence changes are normalized to F_0 of 0 and F_{max} of 10 for GCaMP6s (A) and FGCaMP using excitation at 500 nm (B) and to F_0 of 10 and F_{min} of 0 for FGCaMP using excitation at 402 nm (C). Ca^{2+} concentrations in the mixing chamber are specified in the figure legends.

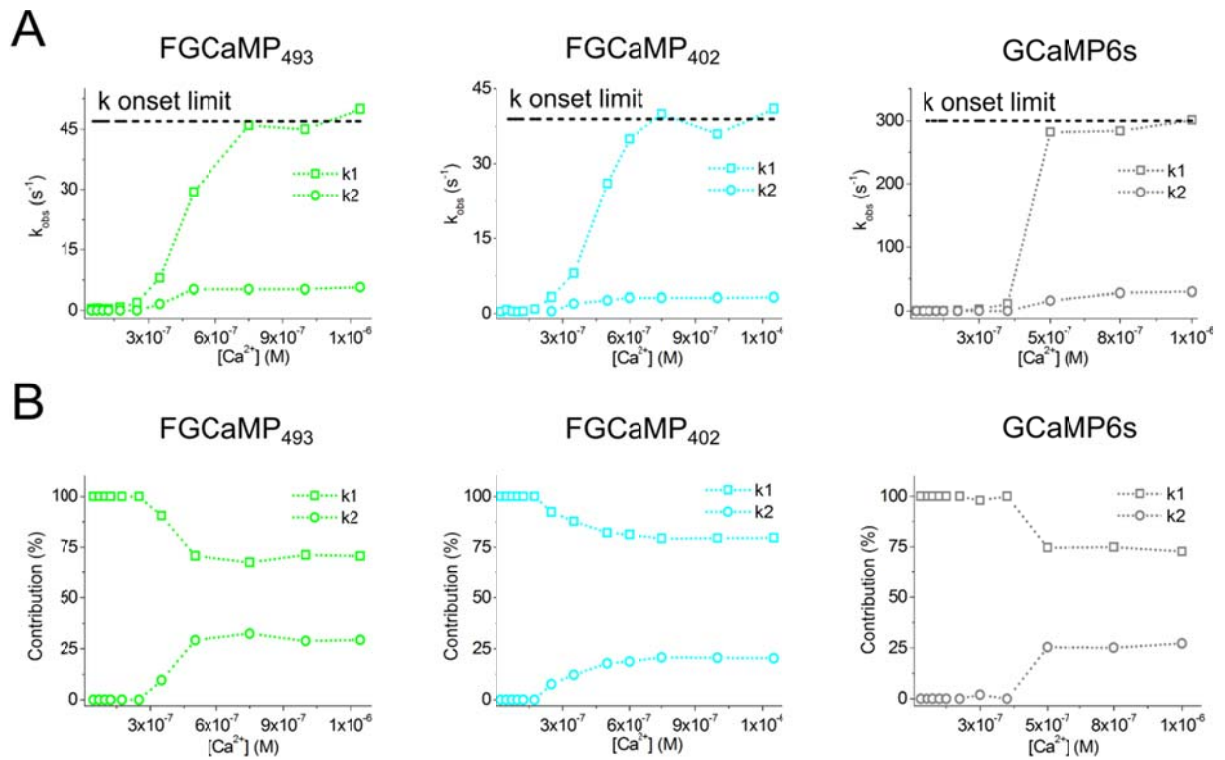


Figure G. Detailed analysis of the onset kinetics for Ca²⁺-binding. (A) Observed association rate constants (k_1 , k_2) obtained by fitting the kinetic curves to double exponentials. (B) Relative contributions of the k_1 and k_2 exponentials. Onset rate limit values (k^{onset} limit) correspond to saturation levels of the observed association rate constants (at $> 600\text{-}800$ nM Ca²⁺ concentrations).

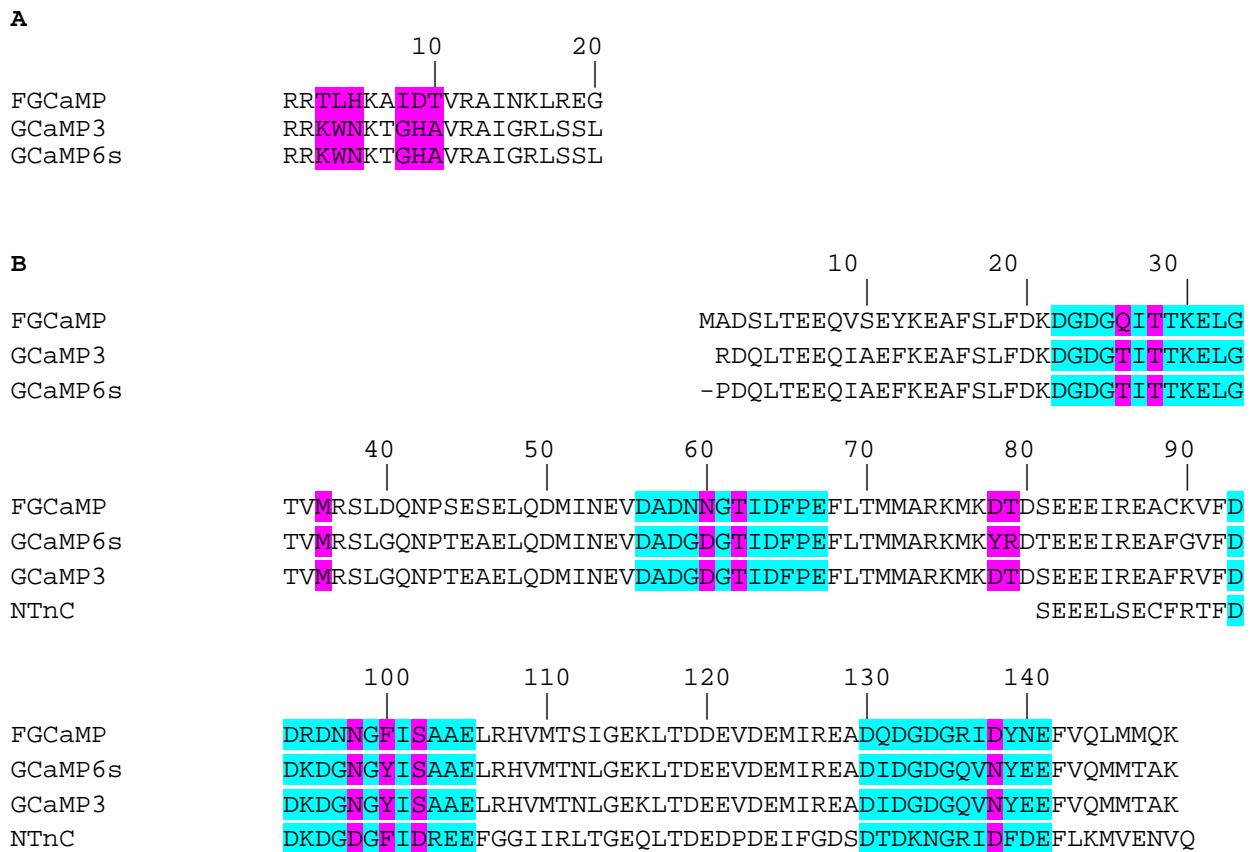
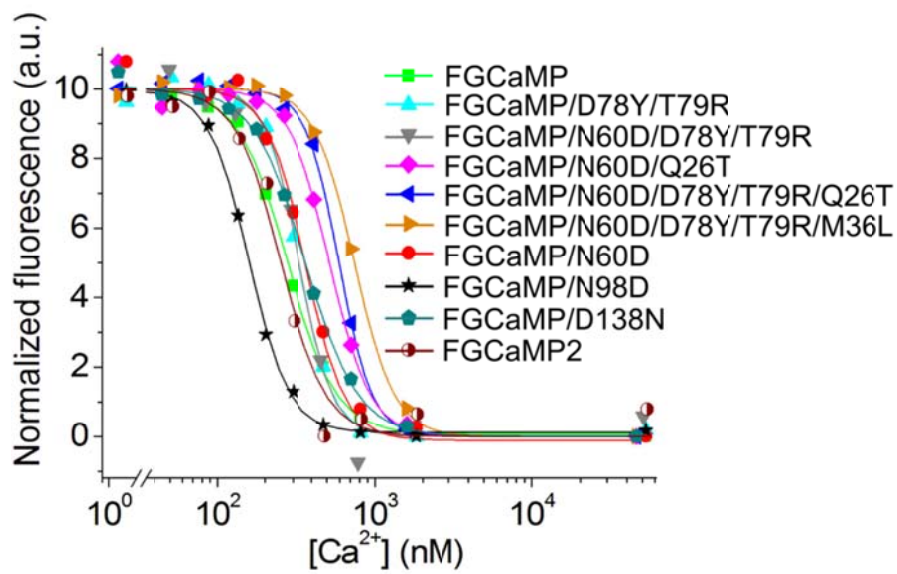


Figure H. Alignment of the amino acid sequences of M13-like peptides and CaMs from FGCaMP and the other calcium indicators. (A) Alignment of peptides from CaM-dependent kinase for FGCaMP, GCaMP3, and GCaMP6s indicators. Mutated randomized residues are highlighted with magenta. (B) Alignment of CaMs from FGCaMP, GCaMP3, GCaMP6s, and NTnC. Four EF1-EF4 hands responsible for calcium-binding are highlighted with cyan, mutated residues are highlighted with magenta. Alignment numbering follows that for GCaMP6s.

A



B

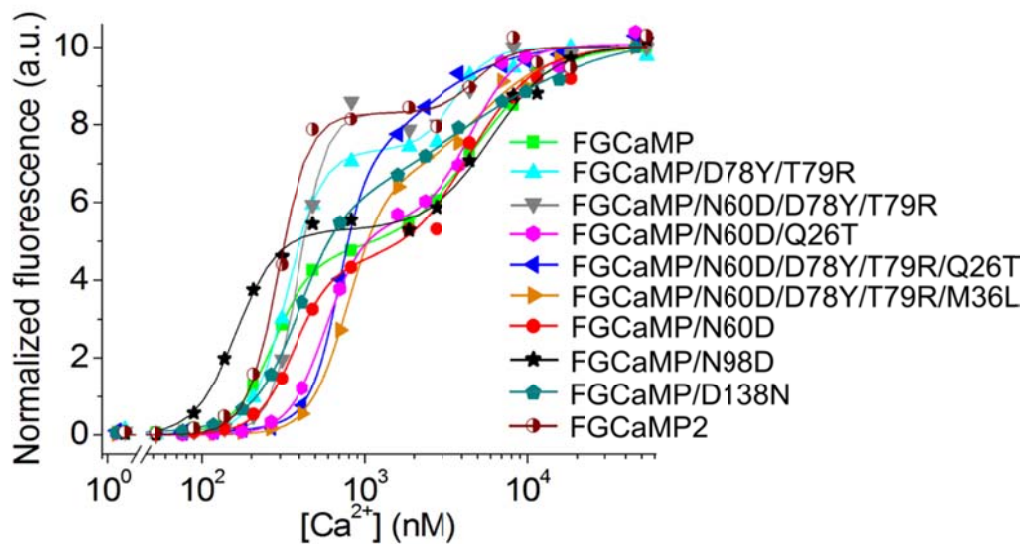
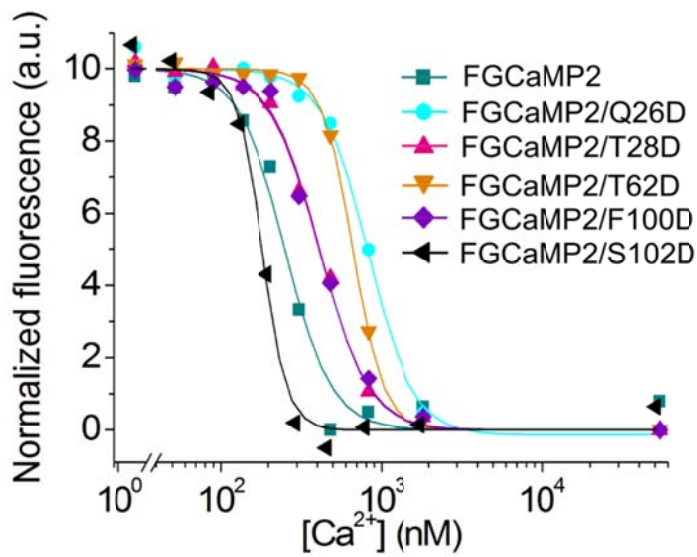


Figure 1. Ca^{2+} titration curves for FGCaMP mutants. (A, B) Ca^{2+} titration curves for 402- (A) and 493-forms (B) of FGCaMP mutants using excitation at 402 and 490 nm, respectively. FGCaMP2 corresponds to FGCaMP/N60D/D78Y/T79R/N98D. Alignment numbering follows that for CaM from GCaMP6s. Fluorescence is normalized to maximal and minimal values. SD corresponds to 20%.

A



B

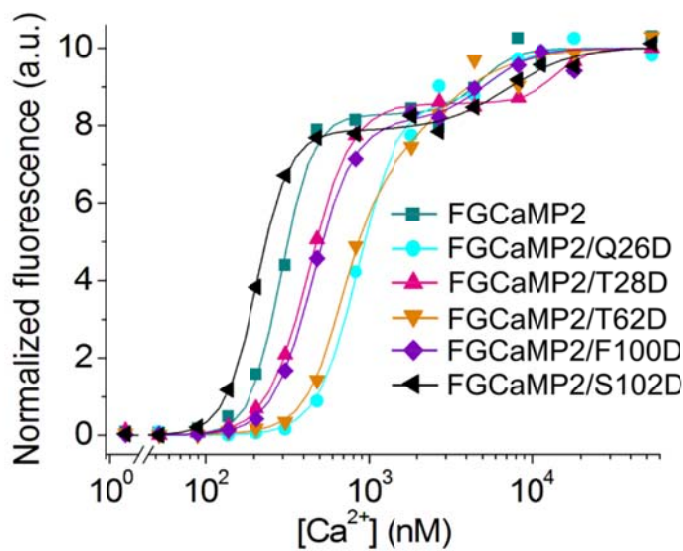


Figure J. Ca^{2+} titration curves for FGCaMP2 mutants with mutations in CaM part. (A, B) Ca^{2+} titration curves for 402- (A) and 493-forms (B) of FGCaMP2 mutants using 402 and 490 nm excitation, respectively. FGCaMP2 corresponds to FGCaMP/N60D/D78Y/T79R/N98D. Alignment numbering follows that for CaM from GCaMP6s. Fluorescence is normalized to maximal and minimal values. SD corresponds to 20%.

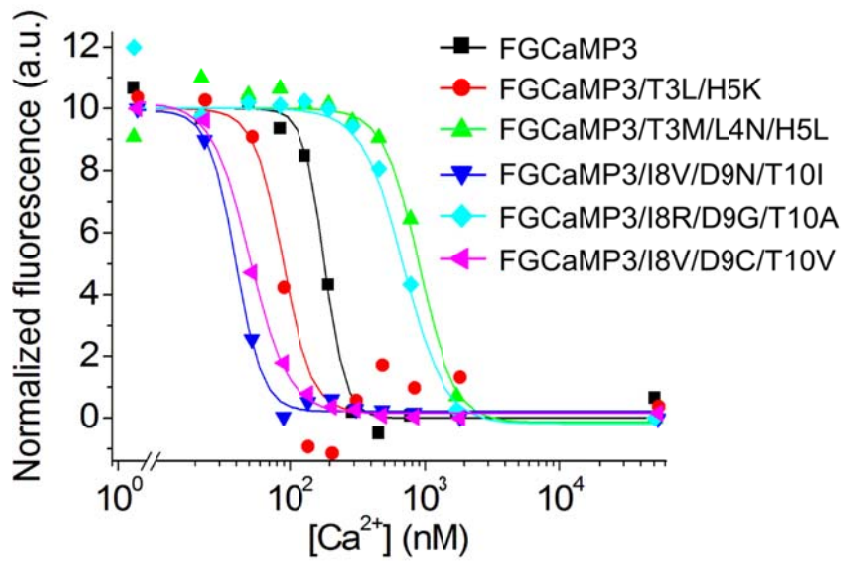
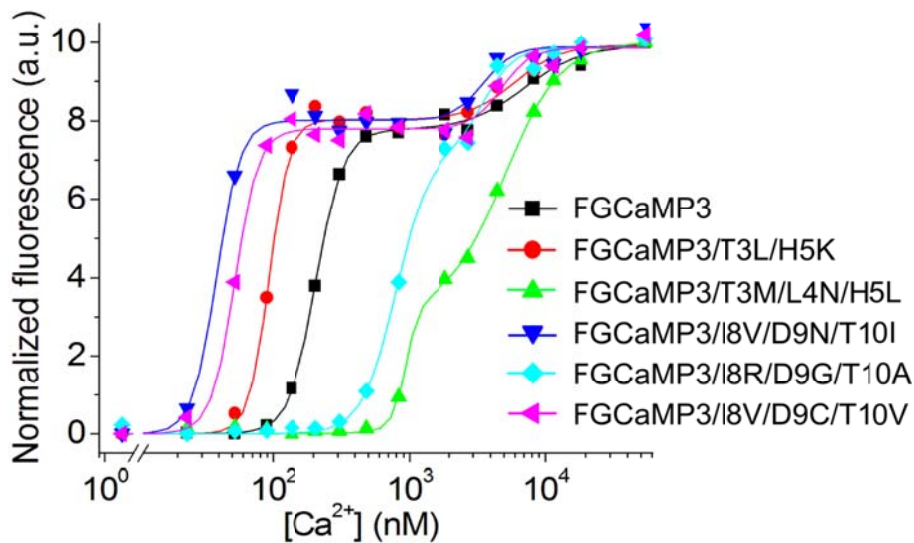
A**B**

Figure K. Ca²⁺ titration curves for FGCaMP3 variants with mutations in the M13-like peptide. (A, B) Ca²⁺ titration curves for 402- (A) and 493-forms (B) of FGCaMP3 mutants using 402 and 490 nm excitation, respectively. FGCaMP3 corresponds to FGCaMP/N60D/D78Y/T79R/N98D/S102D. Alignment numbering follows that for CaM or M13 peptide from GCaMP6s. Fluorescence is normalized to minimal and maximal fluorescence values. SD corresponds to 20%.

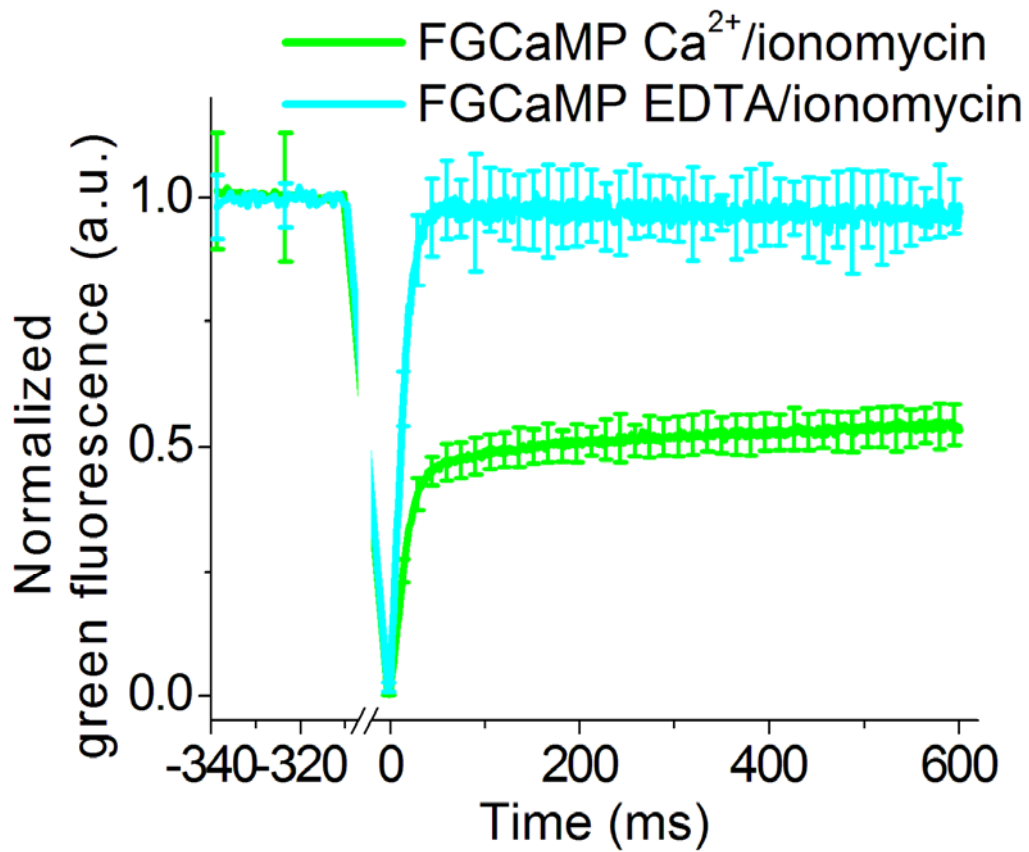


Figure L. Reversible changes in the mobile fraction of the FGCaMP indicator at the transition from high to low Ca²⁺ concentrations in HeLa Kyoto cells studied by FRAP experiments. The graphs illustrate FRAP induced changes in green fluorescence of FGCaMP in response to the addition of 2 mM CaCl₂/5 μM ionomycin (high Ca²⁺ concentrations) followed by washing and addition of 1 mM EDTA/5 μM ionomycin (low Ca²⁺ concentrations). Error bars are standard deviations shown for each 20th dot on plots.

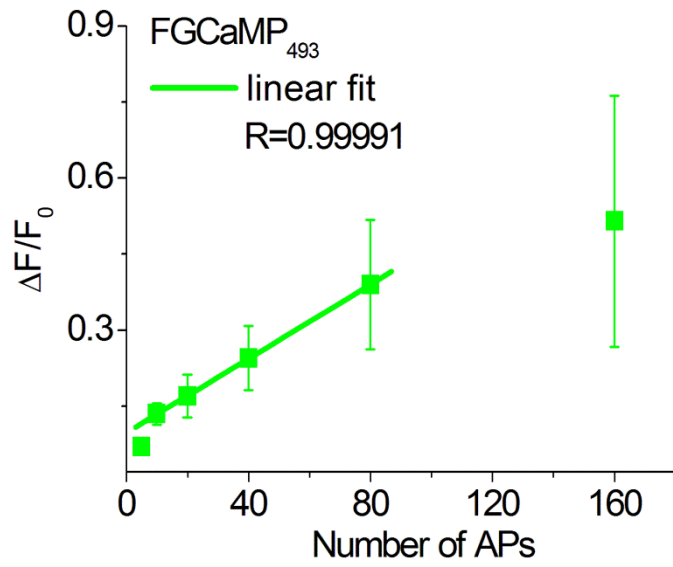


Figure M. Fluorescence changes in response to the external electric field in cultured neurons expressing FGCaMP indicator. Linear region is fitted to a linear equation. APs were induced by electrical pulses of 1 ms, 5 V, and 87 Hz.

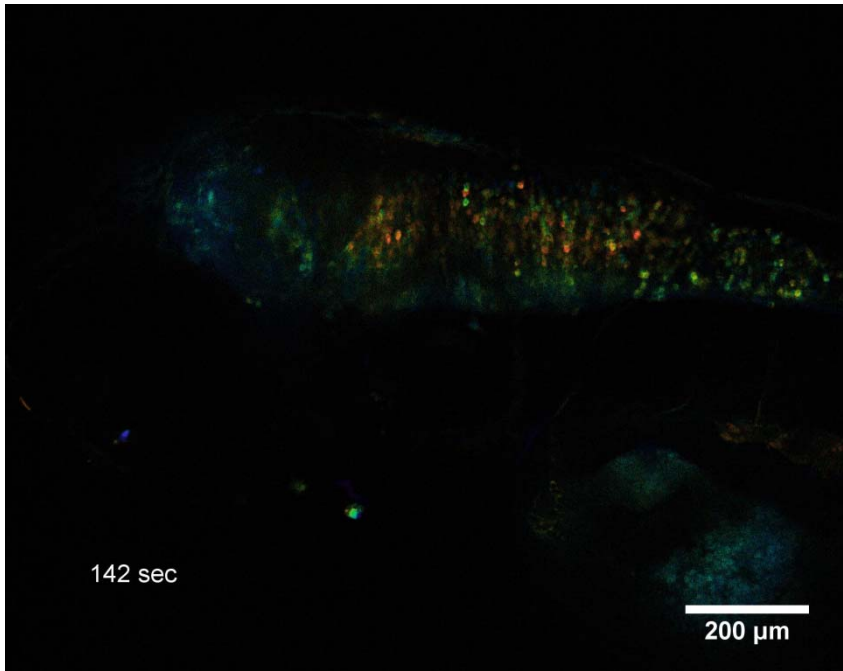


Figure N. Confocal ratiometric calcium imaging with FGCaMP during 4-AP induced neuronal activity in paralyzed larvae embedded in ultra-low-melting agarose gel. Example of frame from S1 Video is shown.

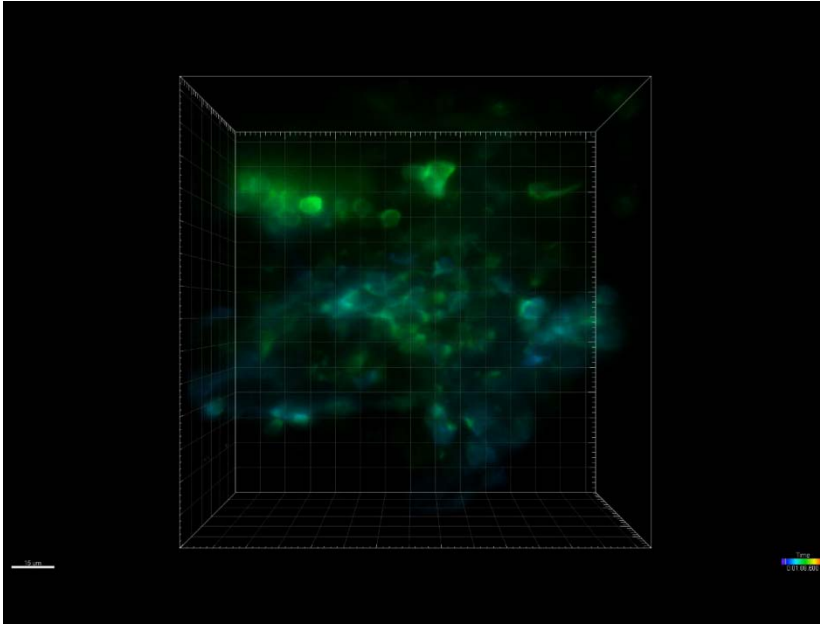


Figure O. Light sheet ratiometric calcium imaging with FGCaMP during 4-AP induced neuronal activity in paralyzed larvae embedded in ultra-low-melting agarose gel. Example of frame from S2 Video is shown.

Table A. Brightness and contrasts for FGCaMP and other ratiometric green and yellow GECIs.

Protein		Brightness	Fluorescence contrast (fold)	Fluorescence Ratio (fold)
FGCaMP	402-form ^{apo}	26	6.9±0.5	101
	493-form ^{sat}	49	14.7±0.6	
GEX-GECO	390-form ^{apo}	6.7 ^a	1.1±0.1	18
	482-form ^{sat}	1 ^a	16.1±0.4	
Ratiometric-pericam ^b	418-form ^{apo}	7.2	ND	10
	494-form ^{sat}	1.9	ND	
Y-GECO ^c	523-form ^{apo}	30	15	200
	413-form ^{sat}	1.2	18	

^a ref [1]. ^b ref [2]. ^c ref [3]

Table B. K_d values and fluorescence contrasts for 402- and 493-forms of FGCaMP and its mutants.

Protein	402-form		493-form			
	K_{d1} (nM)	Contrast (fold)	K_{d1} (nM)	K_{d2} (μ M)	Contrast K_{d1} (fold)	Contrast K_{d2} (fold)
FGCaMP	276 \pm 9	5.1 \pm 0.8	273 \pm 7	4.7 \pm 0.2	9.3 \pm 0.6	1.7 \pm 0.1
FGCaMP/N60D	370 \pm 30	5.5 \pm 0.8	370 \pm 40	4.4 \pm 0.6	9.2 \pm 0.6	1.8 \pm 0.1
FGCaMP/N98D	159 \pm 3	5.8 \pm 0.9	161 \pm 8	6.0 \pm 0.5	8.9 \pm 0.5	1.7 \pm 0.2
FGCaMP/D138N	364 \pm 13	5.4 \pm 0.8	390 \pm 9	5.7 \pm 2.4	9.9 \pm 0.3	1.6 \pm 0.1
FGCaMP/N60D/Q26T	517 \pm 24	3.2 \pm 0.5	575 \pm 32	4.7 \pm 0.2	10.1 \pm 0.1	1.8 \pm 0.1
FGCaMP/D78Y/T79R	330 \pm 8	3.7 \pm 0.6	333 \pm 8	3.6 \pm 0.3	10.0 \pm 0.4	1.3 \pm 0.1
FGCaMP/N60D/D78Y/T79R	332 \pm 20	3.4 \pm 0.5	390 \pm 20	4.9 \pm 1.1	10.7 \pm 0.3	1.2 \pm 0.1
FGCaMP/N60D/D78Y/T79R/Q26T	600 \pm 15	3.4 \pm 0.5	693 \pm 17	3.2 \pm 1.9	11.7 \pm 0.3	1.2 \pm 0.1
FGCaMP/N60D/D78Y/T79R/M36L	743 \pm 23	3.4 \pm 0.5	788 \pm 47	4.6 \pm 1.0	13.0 \pm 0.6	1.3 \pm 0.1
FGCaMP2^a	259 \pm 11	3.3 \pm 0.5	292 \pm 10	4.8 \pm 1.1	11.3 \pm 0.4	1.2 \pm 0.1
FGCaMP2/Q26D	824 \pm 34	4.3 \pm 0.6	857 \pm 33	6.4 \pm 1.5	10.8 \pm 2	1.2 \pm 0.1
FGCaMP2/T28D	412 \pm 13	4.6 \pm 0.7	433 \pm 4	14 \pm 1	13 \pm 1	1.1 \pm 0.1
FGCaMP2/T62D	665 \pm 10	3.7 \pm 0.6	669 \pm 60	2.1 \pm 0.8	9.4 \pm 1.5	1.4 \pm 0.2
FGCaMP2/F100D	415 \pm 19	3.7 \pm 0.6	455 \pm 16	5.3 \pm 1.1	10.2 \pm 0.1	1.2 \pm 0.1
FGCaMP3^a	183 \pm 8	3.0 \pm 0.5	208 \pm 4	7 \pm 1	10.9 \pm 0.2	1.3 \pm 0.1
FGCaMP3/T3L/H5K	90 \pm 20	2.3 \pm 0.4	93 \pm 2	6 \pm 2	6.7 \pm 0.3	1.2 \pm 0.1
FGCaMP3/T3M/L4N/H5L	910 \pm 80	3.3 \pm 0.5	900 \pm 300	5.1 \pm 0.3	4.9 \pm 0.3	2.2 \pm 0.1
FGCaMP3/I8V/D9N/T10I	40 \pm 2	2.7 \pm 0.4	39 \pm 3	3.5 \pm 0.7	6.3 \pm 0.1	1.3 \pm 0.1
FGCaMP3/I8R/D9G/T10A	700 \pm 70	3.0 \pm 0.5	790 \pm 50	3.6 \pm 0.5	4.6 \pm 0.3	1.2 \pm 0.1
FGCaMP3/I8V/D9C/T10V	51 \pm 2	4.6 \pm 0.7	52 \pm 2	4.8 \pm 0.7	7.6 \pm 0.4	1.2 \pm 0.1

^a FGCaMP2 and FGCaMP3 corresponds to FGCaMP/N60D/D78Y/T79R/N98D and FGCaMP2/S102D, respectively.

Alignment numbering follows that for CaM or M13 peptide from GCaMP6s.

Table C. List of primers.

Primer	Primer sequence (5'-3')
CaMA-rv	GTATATTTTCATTGCTCCCCACCCTTTCCGC
CaMN-BglIII	CGAGATCTATGGCCGACTCTCTGACCGAAGAGCAAG
CaMN-HindIII reverse	CCAAGCTTTTTATTTTTGCATCATGAGCTGGACGAACTCGTTG
CaMK-BglIII	CGAGATCTATGTCCGATAAATTGTCCGAAGCCCAAATTC
CaMK-HindIII reverse	CCAAGCTTCTATTTATTAAGTAGGAGATTGGAAAATTCCTTG
M13Fc-BglIII forward	CAGAGATCTAAAAGACGGGCGATCAAGAACAAG
M13Fc reverse	CCGCAACACCTGGAAGACACGCGAGAGACGTCCGATGGCAAGAATCTTGTTCTGATCGCCCCG
M13Fc-cpEGFP forward	GTCTTCCAGGTGTTGCGGNSNNSAACGTCTATATCAAGGCC
M13Fc-cpEGFP reverse	GGCCTTGATATAGACGTTSNNSNCCGCAACACCTGGAAGAC
cpEGFP-CaMF forward	CACAAGCTGGAGTACAACNNSNNSNNSATGGCCGACTCTCTGACCGAAGAGCAAG
cpEGFP-CaMF reverse	CTTGCTCTTCGGTCAGAGAGTCGGCCATSNNSNNSNNGTTGACTCCAGCTTGTG
M13Fk-BglIII forward	CAGAGATCTCGTCGAACGCTGCACAAAGCC
M13Fk reverse	CCCTCGCGGAGCTTGTGATGGCGCGGACGGTATCGATGGCTTTGTGCAGCGTTCG
M13Fk-cpEGFP forward	CAACAAGCTCCGCGAGGGANNSNNSAACGTCTATATCAAGGCC
M13Fk-cpEGFP reverse	GGCCTTGATATAGACGTTSNNSNNTCCCTCGCGGAGCTTGTG
M13KPk-BglIII forward	CAGAGATCTAAGAAAGTGGTACTCAGAAATAAG
M13KPk reverse	GGAGAACTTGATACATCCTGGATACTCTTCCAATTGCCAGAATCTTATTTCTGAGTACCACCTTC
M13KPk-cpEGFP forward	GGATGTATCAAGTTCTCCGTNNSNNSAACGTCTATATCAAGGCC
M13KPk-cpEGFP reverse	GGCCTTGATATAGACGTTSNNSNACGGAGAACTTGATACATCC
cpEGFP-CaMKP forward	CACAAGCTGGAGTACAACNNSNNSNNSATGTCCGATAAATTGTCCGAAGCCCAATTTTC
cpEGFP-CaMKP reverse	GAAATTTGGGCTTCGGACAATTTATCGGACATSNNSNNSNNGTTGACTCCAGCTTGTG
M13KPk-BglIII forward	CAGAGATCTAGATCCAAGTTCAAGCAAG
M13KPk reverse	GTTCTTCAATCTGTTTTGCATCTTGACAATCTCGATGACTTGCTTGAACCTTGGATC
M13KPk-cpEGFP forward	GCAAAACAGATTGAAGAACCTCNSNNSAACGTCTATATCAAGGCC
M13KPk-cpEGFP reverse	GGCCTTGATATAGACGTTSNNSNNGAGGTTCTTCAATCTGTTTTGC
FCaMP-M36L forward	CAAGGAGCTCGGCACTGTGCTGCGCTCCCTTGACCAGAAC
FCaMP-M36L reverse	GTTCTGGTCAAGGGAGCGCAGCACAGTGCCGAGCTCCTTG
FCaMP-N60D forward	GAGGTTGACGCTGACAACGACGGAACGATCGACTTCC
FCaMP-N60D	GGAAGTCGATCGTTCCGTGCTGTCAGCGTCAACCTC

<i>reverse</i>	
<i>FCaMP-78YR forward</i>	GATGGCTCGTAAGATGAAGTACAGAGACACCGAGGAGGAAATCCGCG
<i>FCaMP-78YR reverse</i>	CGCGGATTTCTCCTCGGTGTCTGTACTTCATCTTACGAGCCATC
<i>FCaMP-Q26T forward</i>	CAAGGATGGCGATGGCACGATCACCACCAAGGAGCTC
<i>FCaMP-Q26T reverse</i>	GAGCTCCTTGGTGGTGATCGTGCCATCGCCATCCTTG
<i>FCaMP-N98D forward</i>	GTCTTCGACCGCGACAACGATGGTTTTATCTCCGCCGCG
<i>FCaMP-N98D reverse</i>	CGCGGCGGAGATAAAACCATCGTTGTCGCGGTCTGAAGAC
<i>FCaMP-D138N reverse</i>	GAGCTGGACGAACTCGTTGTAGTTGATGCGGCCATCACCGTC
<i>FC-102D forward</i>	GACAACGATGGTTTTATCGACGCCGCGGAGCTGCGCCAC
<i>FC-102D reverse</i>	GTGGCGCAGCTCCGCGCGTTCGATAAAACCATCGTTGTC
<i>FC-BglII-M13NNS1 forward</i>	GGCAGATCTATGCGTAGCCGTCGANNSNNSNNSAAAGCCATCGATACCGTC
<i>FC-BglII-M13NNS2 forward</i>	GGCAGATCTATGCGTAGCCGTCGAACGCTGCACAAAGCCNNSNNSNNSGTCC GCGCCATCAACAAG
<i>G-FCaMP-BamHI-NheI forward</i>	TGGGGATCCGGCTAGGCCACCATGCGTCTGAACGCTGCACAAAGCC
<i>GEX-GECO-BglII forward</i>	CAGAGATCTATGGTTCGACTCATCACGTC
<i>GEX-GECO-EcoRI reverse</i>	CAGGAATTCTCACTTCGCTGTCATCATTTG

References

1. Zhao Y, Araki S, Wu J, Teramoto T, Chang YF, Nakano M, et al. (2011) An expanded palette of genetically encoded Ca²⁺ indicators. *Science* 333: 1888-1891.
2. Nagai T, Sawano A, Park ES, Miyawaki A (2001) Circularly permuted green fluorescent proteins engineered to sense Ca²⁺. *Proceedings of the National Academy of Sciences of the United States of America* 98: 3197-3202.
3. Zhao Y, Abdelfattah AS, Ruangkittisakul A, Ballanyi K, Campbell RE, Harrison DJ (2014) Microfluidic cell sorter-aided directed evolution of a protein-based calcium ion indicator with an inverted fluorescent response. *Integrative biology : quantitative biosciences from nano to macro* 6: 714-725.